Fang, Y., Ferrie, A., Fontaine, N. & Yuen, P. Characteristics of dynamic mass redistribution of EGF receptor signaling in living cells measured with label-free optical biosensors....

ARTICLE *in* ANALYTICAL CHEMISTRY · OCTOBER 2005

Impact Factor: 5.64 · DOI: 10.1021/ac050887n · Source: PubMed

Anal. Chem. **2005,** *77,* 5720−5725

Characteristics of Dynamic Mass Redistribution of Epidermal Growth Factor Receptor Signaling in Living Cells Measured with Label-Free Optical Biosensors

Ye Fang,* Ann M. Ferrie, Norman H. Fontaine, and Po Ki Yuen

Biochemical Technologies, Science and Technology Division, Corning Incorporated, Sullivan Park, Corning, New York 14831

This paper reported the identification of a novel optical signature for epidermal growth factor (EGF) receptor signaling in human epidermoid carcinoma A431 cells mediated by EGF. The optical signature was based on dynamic mass redistribution (DMR) in living cells triggered by EGFR activation, as monitored in real time with resonant waveguide grating biosensors. Analysis of the modulation of the EGF-induced DMR signals by a variety of known modulators provided links of various targets to distinct steps in the cellular responses. Results showed that the dynamic mass redistribution in quiescent A431 cells mediated by EGF required EGFR tyrosine kinase activity, actin polymerization, and dynamin and mainly proceeded through MEK. The DMR signals obtained serve as integrated signatures for interaction networks in the EGFR signaling.

The combinatorial integration of signaling pathways mediated through a specific molecule in response to stimuli plays an important role in the specificity of cellular responses and cell functions, as best exampled by the signaling of epidermal growth factor (EGF) receptor.[1−4] Upon ligand binding, the EGFR becomes dimerized and activated through the autophosphorylation of the receptor on tyrosine residues in the cytoplasmic domain, thus initiating a number of intracellular signals by interacting with distinct signaling proteins. The Ras/MAPK pathway mediated through EGFR is well known to proceed via the signaling proteins Shc, Grb2, Sos, Ras, Raf, MEK, ERK, and ERK/MAPK. The MAPK pathway regulates a diverse array of cellular functions including cell proliferation, survival, motility, differentiation, and cycling. However, the specificity of cell responses is largely determined by the integration of signaling network interactions and depends on the cellular context.[3]

Traditional cell-based methods rely on the measurements of a single cellular event, such as second-messenger generation (e.g., Ca^{2+} flux, cAMP level changes), the translocation of a particular target tagged with a fluorescence label, or the expression of a reporter gene.[5−6] These methods can provide functional, kinetic cell-based information on the cellular consequences of target−compound interaction, including drug mechanisms of action, efficacy, selectivity, and cytotoxicity. However, these methods tend to fail to generate information relating to the overall cellular responses, because of the complexity of cell function as well as the dependence of specific cell responses on the integration of a multitude of signaling pathways. In addition, the use of either labels or artificial manipulations could contribute in an adverse way to elucidating the real cellular physiology of the targets studied.

Several label-free biosensor technologies have been applied to monitor cell activity, including the activation of G protein-coupled receptors by surface plasmon resonance,[7] the effect of compounds on cell growth by resonant waveguide grating (RWG),[8] and the signaling of cell surface molecules based on the cell−substrate impedance.[9] In this paper, we applied the RWG biosensor to monitor the EGF-induced dynamic mass redistribution in human epidermoid carcinoma A431 cells and for the first time studied the signaling networks that contribute to the mass redistribution signal observed.

MATERIALS AND METHODS

Materials. EGF, cytochalasin B, latrunculin A, vinblastine, wortmainnin, phalloidin, and nocodazole were purchased from Sigma Chemical Co. (St. Louis, MO). AG1478, PP1, PD98059, U0126, SB203580, SB202190, SP600125, KT5720, KT5823, KN62, GF109203x, cell-permeable dynamin inhibitor peptide control (DIPC), (*R*)-(−)-rolipram, Ro 20-1724, zardaverine, and milrinone were purchased from Tocris Chemical Co. (St. Louis, MO). Tetramethylrhodamine-labeled EGF (TMR-EGF) and Texas Red-labeled phalloidin (TR-phalloidin) were obtained from Molecular Probes (Eugene, OR). Corning Epic 96-well biosensor microplates were obtained from Corning Inc. (Corning, NY) and cleaned by

* To whom correspondence should be addressed. E-mail: fangy2@corning.com. Tel: 607-9747203. Fax: 607-9745957.

(1) Schlessinger, J. *Cell* **2000**, *103*, 211−225.
(2) Schoeberl, B.; Eichler-Jonsson, C.; Gilles, E. D.; Muller, G. *Nat. Biotechnol.* **2002**, *20*, 370−375.
(3) Kolch, W.; Calder, M.; Gilbert, D. *FEBS Lett.* **2005**, *579*, 1891−1895.
(4) Wetzker, R.; Bohmer, F.-D. *Nat. Rev. Mol. Cell Biol.* **2003**, *4*, 651−657.
(5) Milligan, G. *Drug Discovery Today* **2003**, *8*, 579−585.
(6) Hu, C.-D.; Kerppola, T. K. *Nat. Biotechnol.* **2003**, *21*, 539−545.
(7) Hide, M.; Tsutsui, T.; Sato, H.; Nishimura, T.; Morimoto, K.; Yamamoto, S.; Yoshizato, K. *Anal. Biochem.* **2002**, *302*, 28−37.
(8) Cunningham, B. T.; Li, P.; Schulz, S.; Lin, B.; Baird, C.; Gerstenmaier, J.; Genick, C.; Wang, F.; Fine, E.; Laing, L. *J. Biomol. Screening* **2004**, *9*, 481−490.
(9) Ciambrone, G. J.; Liu, V. F.; Lin, D. C.; McGuinnes, R. P.; Leung, G. K.; Pitchford, S. *J. Biomol. Screening* **2004**, *9*, 467−480.

10.1021/ac050887n CCC: $30.25
Published on Web 08/06/2005

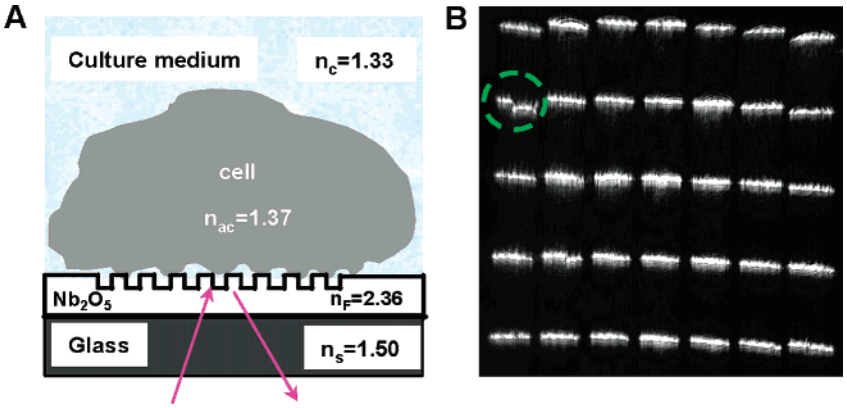

Figure 1. (A) Schematic drawing showing the configuration of the optical biosensor for cell sensing. The sensor consists of a thin film of Nb_2O_5 with a high refractive index (n_F = 2.36) on a glass substrate with an index of n_s = 1.50. The cell monolayer on the waveguide film has an overall refractive index of n_A=1.37, and a surrounding medium has an index of ~1.33 (n_c). (B) An actual resonant band image of 5 rows of 7 sensors in a 96-well sensor microplate containing living cells obtained using our arrayed angular interrogation system. The broken circle indicated that the cell density was not even across this specific sensor, which was confirmed by light microscopic imaging.

exposure to high-intensity UV light (UVO cleaner, Jelight Co. Inc., Laguna Hills, CA) for 6 min before use.

Cell Culture. Both human epidermoid carcinoma A431 and Chinese hamster ovary (CHO) cells were obtained from American Type Cell Culture. A431 cells were grown in Dulbecco's modified Eagle's medium supplemented with 10% fetal bovine serum (FBS), 4.5 g/L glucose, 2 mM glutamine, and antibiotics. CHO cells were grown in Kaighn's modification of Ham's F12 medium (F-12K) supplemented with 10% FBS, 2 mM L-glutamine, 3 mg/mL sodium bicarbonate, and antibiotics. For cell culture, ~(3−7.5) × 10^4 cells suspended in 200 μL of the corresponding medium containing 10% FBS were placed in each well of a 96-well biosensor microplate and were cultured at 37 °C under air/5% CO_2 until ~95% confluency was reached (~2−4 days). The cells were then subject to starvation with the corresponding medium with or without 0.1% FBS for a given time. Because the biological status of cells (e.g., cell viability, confluency, and degree of adhension) could significantly impact the measurement of mass redistribution, we inspected the quality of cells using both light microscopy and the optical system. The optical system allows one to collect the resonant band image and peak of each sensor, which are sensitive to the cell quality (data not shown; ref 10).

Before assays, the cells were washed twice and maintained with 100 μL of the corresponding medium. Afterward, the sensor microplate containing cells was placed into an arrayed angular interrogation system, and the cell responses were recorded before and after addition of a solution. For compound studies, the cells in each well were pretreated with a corresponding compound solution of 50 μL or the HBSS buffer solution until a steady phase (i.e., no obvious mass redistribution) was reached (generally within 1 h), before the EGF solution of 50 μL was introduced. The HBSS buffer solution served as a control so that any effect, besides the compound or EGF, can be monitored and minimized by delaying the sequential treatment. Since the baseline of the responses varied from well to well, we normalized the EGF response in the absence and presence of a compound at the time when the cells were in steady state before EGF stimulation.

Resonant Waveguide Grating Biosensor System. The Corning Epic angular interrogation system with transverse magnetic or *p*-polarized TM_0 mode was used for all studies. This system consists of a launch system for generating an array of light beams such that each illuminates a RWG sensor, with a dimension of ~200 μm × 3000 μm, and a CCD camera-based receive system for recording changes in the angles of the light beams reflected from these sensors. The arrayed light beams were obtained through a beam splitter and diffractive optical lenses. This system allows up to 49 sensors in a microplate (in a 7 × 7 well sensor array) to be simultaneously sampled every 3 s. Unlike SPR, which is fine-tuned for affinity screening against the surface-bound "receptors" and generally uses a parallel flow chamber to continuously deliver bioassay solution, the current system remains static and allows the gentle introduction of solution(s) using an on-board liquid handling system during the assay, so that it minimized the unwanted effect of fluid movements on the cells.[11−13] Because of the unique design, each sensor gives rise to a resonant band (Figure 1B) that can be divided into multiple segments for data collection and analysis. The segments having no cells serve as intrawell self-referencing to filter out any unwanted effects as they occur.

The RWG sensors are thermally sensitive, meaning that any difference in temperature between the compound solution and the cell medium could complicate the cell responses. To minimize or eliminate such an effect, all solutions had been equilibrated for ~3 h inside the detection system before being applied to the cells. In addition, all studies were carried out at room temperature in order to minimize the effect of temperature fluctuation and evaporative cooling. The unit of the responses indicated throughout this paper was a change in pixel of the central position of the resonant band of each sensor as imaged by the CCD camera; 1 unit equals to ~45-pm shift in wavelength, a common parameter used for surface plasmon resonance as well as the RWG biosensor.

Fluorescence Imaging. For actin filament staining, cells were grown on glass coverslips, chased with 16 nM EGF at room

(10) Horvath, R.; Voros, J.; Graf, R.; Fricsovszky, G.; Textor, M.; Lindvold, L. R.; Spencer, N. D.; Papp, E. *Appl. Phys. B* **2001**, *72*, 441−447.
(11) Tzima, E.; del Pozo, M. A.; Kiosses, W. B.; Mohamed, S. A.; Li, S.; Chien, S.; Schwartz, M. A. *EMBO J.* **2001**, *20*, 4639−4647.
(12) Orr, A. W.; Sanders, J. M.; Bevard, M.; Coleman, E.; Sarembock, I. J.; Schwartz, A. *J. Cell Biol.* **2005**, *169*, 191−2002.
(13) Wang, Y.; Botvinick, E. L.; Zhao, Y.; Berns, M. W.; Usami, S.; Tsien, R. Y.; Chien, S. *Nature* **2005**, *434*, 1040−1045.

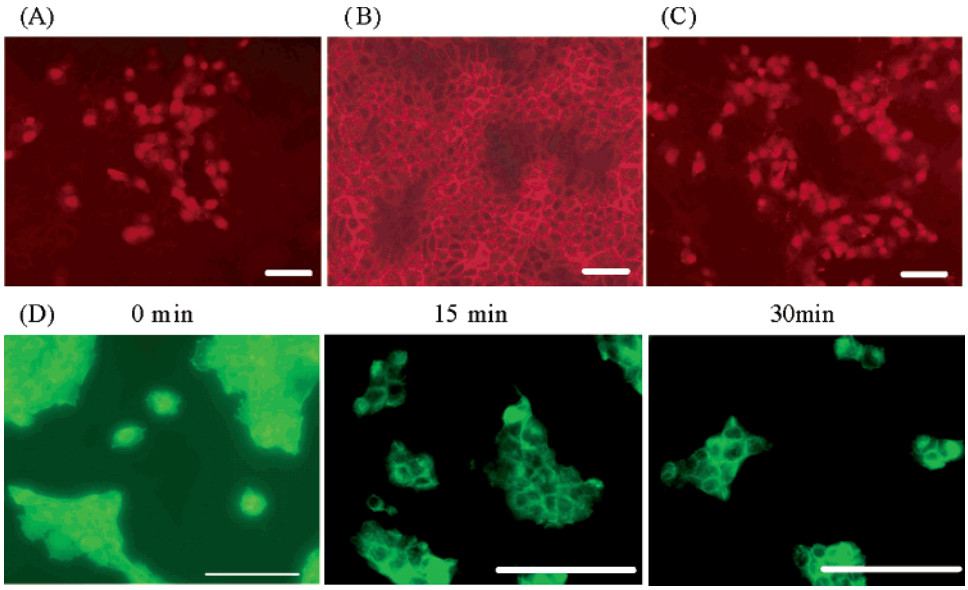

Figure 2. EGF-induced EGFR internalization and morphological changes of A431 cells at room temperature (22 °C). (A) Fluorescence image of proliferating A431 cells (10% FBS) after staining with 16 nM TMR-EGF followed by stripping away the surface-bound TMR-EGF with the acidic solution at 4 °C. (B) Fluorescence image of quiescent A431 cells (0.1% FBS, 20 h) after staining with 16 nM TMR-EGF. (C) Fluorescence image of the quiescent A431 after staining and subsequently stripping away the surface-bound TMR-EGF with the acidic solution at 4 °C. (D) Quiescent A431 cells treated with 16 nM EGF for the indicated times were examined using fluorescence microscopy after fixation and stained with TR-phalloidin. The bar represents 40 μm.

temperature for a certain time, fixed with 4% paraformaldehyde, permeabilized in phosphate-buffered saline containing 0.2% Triton, and blocked with 1% bovine serum albumin. Cells were incubated with 0.5 μM TR-phalloidin for 1 h at room temperature and washed. After final washes and mounting, cells were examined with a 20 × or 30 × objective. For receptor endocytosis studies, cells were grown on the sensor microplate, incubated with 16 nM TMR-EGF at room temperature for 30 min, and directly imaged. Afterward, the plates were immediately washed twice with ice-cold saline and washed with ice-cold acidic stripping buffer (100 mM acetic acid, 150 mM NaCl, pH 3) for 1 min. The cells were then washed with HBSS three times and imaged. A Zeiss Axioplan fluorescence microscope was used to collect all fluorescence and light images.

RESULTS AND DISCUSSIONS

To study EGFR signaling, we developed a protocol of ligand-induced dynamic mass redistribution (DMR) in living cells using the RWG biosensors (Figure 1). The RWG biosensor is an evanescent wave-based sensor and is capable of detecting refractive index changes in the vicinity of the sensor surface.[14] The change in refractive index is directly proportional to mass redistribution. Since the amplitude of the evanescent wave penetrating into the cells and their surrounding medium decays exponentially with increasing distance from the sensor surface, a target or complex of certain mass contributes more to the overall response when the target or complex is closer to the sensor surface as compared to when it is further from the sensor surface. Because of the small penetration depth (also termed as sensing volume, ~112 nm) of our sensors, only the bottom portion of the cells was monitored. Because the endogenous macromolecules are highly organized within the cytoplasm of mammalian cells and not free to diffuse over large distance,[15−16] stimulation-triggered movement of target molecules or molecular assemblies into or out of the sensing volume appears not random and chaotic. Such movements could lead to a change in local refractive index, which can be detected by the biosensor. A net increase in mass within the penetration depth results in an increase in the angle of the reflected light; vice versa, a net decrease in mass leads to a decrease in the angle.

Upon EGF stimulation, there are many events leading to mass redistribution in A431 cells—a cell line endogenously overexpresses EGFRs.[17] For example, EGFR activation leads to the recruitment of intracellular component(s) to the activated receptor, the movement of the resultant complexes, and the rearrangement of cytoskeleton structure that ultimately results in chemokinetic motility. When such movements or changes occur in the cell near the sensor surface, a DMR signal could be generated. Such signal should offer an integrated signature for EGFR activation. Figure 2 showed two cellular responses that could result in significant mass redistribution. Stimulation of quiescent A431 cells with TMR-EGF at room temperature resulted in receptor internalization as revealed by the location of internalized TMR-EGF molecules with the activated receptors after stripping away the surface-bound labeled EGF. As expected, quiescent cells have much higher cell surface and internalized receptors than proliferating cells. EGF stimulation also caused actin rearrangement as shown by the staining patterns of actin filaments with TR-phalloidin. Actin remodeling started to change after ~15 min of EGF treatment and became more dramatic for longer stimulation, as indicated by the rim of filamentous actin at the edge of the cell. Both events

(14) Tiefenthaler, K.; Lukosz, W. *J. Opt. Soc. Am. B* **1989**, *6*, 209−220.

(15) Srere, P. A. *Trends Biochem. Sci.* **2000**, *25*, 150−153.

(16) Hudder, A.; Nathanson, L.; Deutscher, M. P. *Mol. Cell. Biol.* **2003**, *23*, 9318−9326.

(17) Barnes, D. W. *J. Cell. Biol.* **1982**, *93*, 1−4.

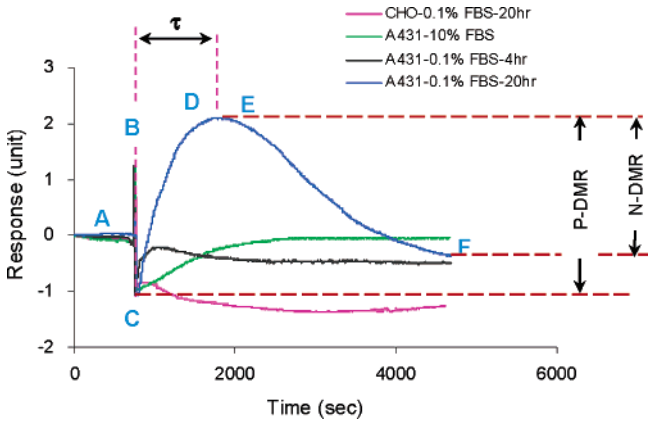

Figure 3. Cell-specific DMR signals in response to EGF stimulation. The DMR responses of adherent A431 cells cultured under three different conditions were compared with that of quiescent CHO cells. Before stimulation with 8 nM EGF, the cells were treated with 1× HBSS (1× regular Hank's balanced salt solution, 20 mM HEPES buffer, pH 7.0, 2.5mM probenecid) twice, each 25 μL, and separated by 15 min such that the cells become resistant to the medium changes and reach a steady state, as indicated by a prolonged net-zero DMR response. Note that there is a rapid response change in signal, lasting for less than 20 s (point B to C), which occurs upon the introduction of 50 μL of EGF solution into the well. This rapid change is due primarily to a bulk index change, which temporarily overwhelms any DMR signal when occurring.

observed here exhibited similar kinetics compared to those at 37 °C (data not shown; refs 18−20).

To study the mass redistribution triggered by EGF, the angular integration system was used to monitor in real time the EGF-induced DMR, which was manifested by angular shifts of the reflected light from the sensor (Figure 3). Results showed that EGF-induced DMR responses of A431 cells strongly depend on the culture condition. The response of quiescent cells (0.1% FBS, 20 h) consists of three distinct, sequential phases: (i) a positive phase with increased signal (P-DMR) (point C to D in Figure 3), (ii) a transition phase (D to E), and (iii) a decay phase (N-DMR) (E to F). A431 cells treated with 0.1% FBS for only 4 h gave rise to similar response but with altered kinetics and much smaller amplitudes, compared to the quiescent cells. Conversely, proliferating A431 cells (10% FBS) only led to a P-DMR event upon EGF stimulation. Furthermore, no significant responses were observed for either quiescent or proliferating CHO cells, which have no endogenous EGFR.[21] These results suggested that the EGF-induced DMR signals are EGFR dependent. Because of the rapid diffusion of EGF in medium and the use of saturated concentrations of EGF, complete phosphorylation of cell surface EGFRs should occur within tens of seconds, accomplished through signal propagation.[2,22−23] Thus, we hypothesized that the P-DMR signal mainly resulted from the recruitment of intracellular components to activated receptors, whereas cell detachment and receptor internalization[18−20] are two major contributors to the N-DMR event.

To address the specificity of EGFR activation, EGF dose responses were examined. Results showed that the EGF-induced responses are saturable (Figure 4A). The higher the EGF concentration, the greater are the amplitudes of both the P-DMR and N-DMR signals, the faster are both the P-DMR and N-DMR events, and the shorter is the transition time τ from the P-DMR to N-DMR event. The amplitudes of the N-DMR event were clearly saturable to EGF, resulting in a k_d of ~1.45 nM (Figure 4B). The transition time τ in seconds decreased exponentially with the increasing concentration C in nM of EGF, yielding an EC_{50} of ~4.5 nM (Figure 4C):

$$\tau(C) = 946e^{-0.144C} + 1130 \quad (1)$$

The decay of the N-DMR signal can be fitted with nonlinear regression, resulting to a saturable decay constant κ with a K_d of 5.76 nM (Figure 4d). These results confirmed that the DMR signal is dependent on EGFR activation.

To study the role of EGFR phosphorylation in the DMR response, a potent and specific EGFR kinase inhibitor, AG1478, and a Src-family tyrosine kinase inhibitor, PP1, were used. To accelerate the kinetics of cell response, A431 cells were starved in a medium without FBS for 20 h prior to EGF exposure. The pretreatment of A431 cells with AG1478 resulted in a dose-dependent suppression on the EGF response with an IC_{50} of ~194 nM (Figure 5A and B). In contrast, PP1 only partially attenuated the EGF-induced response with a slightly delayed transition time (data not shown). These data indicated that EGFR tyrosine kinase activity is required for the EGF-induced DMR changes.

To elucidate the mechanism of the EGF-induced DMR, quiescent A431 cells were pretreated with a panel of modulators until a steady state was reached (generally within 1 h) prior to exposure to 32 nM EGF. The inhibitors were chosen based on their known pharmacological properties and affinities to distinct targets. The concentration of each modulator used was based on its EC_{50} reported in the literature such that maximum inhibitions of the specific targets are achieved with minimal cross talk to other targets.

EGF regulates cell proliferation and differentiation using, at least in part, MAPKs as downstream signals.[1−3] Furthermore, ERK activation seems to represent a global, negative signal downstream of EGFR activation, which may be important in cell detachment from the substrate.[24] Thus, we examined the effect of inhibitors targeting the Ras/MAPK pathways, including the MEK inhibitors PD98059 and U0126, the p38 MAPK inhibitors SB203580 and SB20219, and the JNK inhibitor SP600125. U0126 significantly suppressed both the P-DMR and N-DMR signals with a delayed time τ (Figure 5C), while the low-affinity MEK inhibitor PD 98059 attenuated the responses to less extent (data not shown). Previous studies have shown that inhibition of MEK1/2 prevents EGF-induced cell detachment and movement[18] but not the receptor endocytosis, and blockage of the endocytosis of activated MEK

(18) Lu, Z.; Jiang, G.; Blume-Jensen, P.; Hunter, T. *Mol. Cell Biol.* **2001**, *21*, 4016−4031.
(19) Danjo, Y.; Gipson, I. K. *J. Cell Sci.* **1998**, *111*, 3323−3332.
(20) Resat, H.; Ewald, J. A.; Dixon, D. A.; Wiley, H. S. *Biophys. J.* **2003**, *85*, 730−743.
(21) Livneh, E.; Prywes, R.; Kashles, O.; Reiss, N.; Sasson, I.; Mory, Y.; Ullrich, A.; Schlessinger, J. *J. Biol. Chem.* **1986**, *261*, 12490−12497.
(22) Verveer, P. J.; Wouters, F. S.; Reynolds, A. R.; Bastiaens, P. I. *Science* **2000**, *290*, 1567−1570.
(23) Kempiak, S. J.; Yip, S.-C.; Backer, J. M.; Segall, J. E. *J. Cell Biol.* **2003**, *162*, 781−787.
(24) Glading, A.; Chang, P.; Lauffenburger, D. A.; Wells, A. *J. Biol. Chem.* **2000**, *275*, 2390−2398.

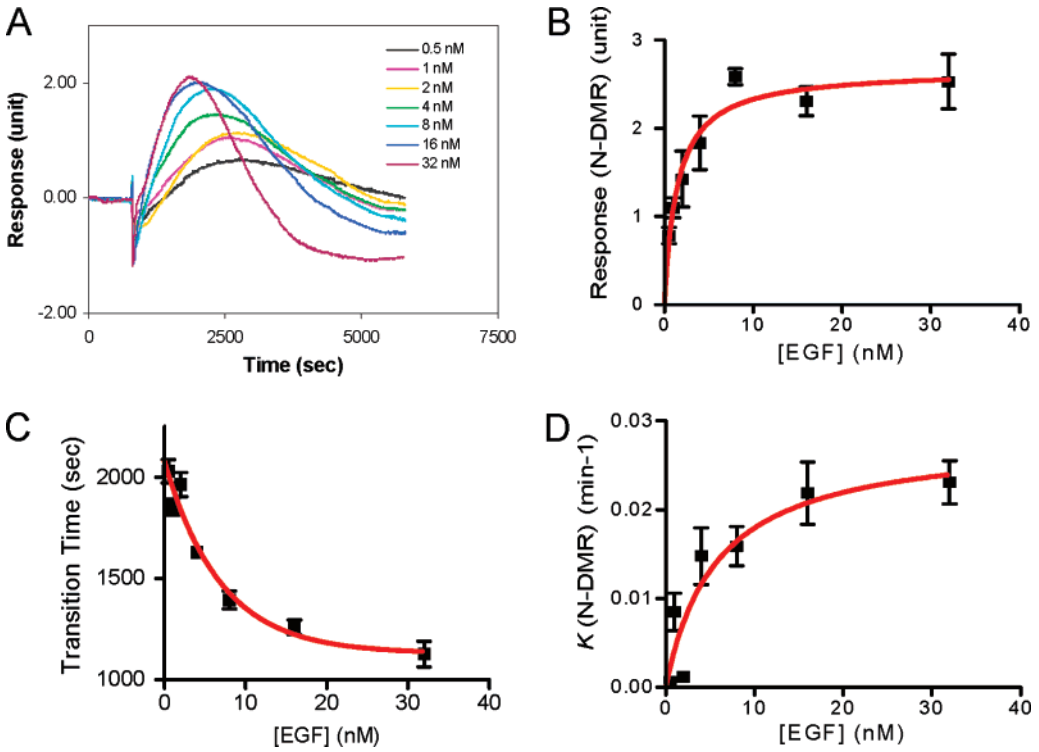

Figure 4. Dose-dependent responses of quiescent A431 cells induced by EGF. (A) Real-time kinetics of the cell responses induced by different concentrations of EGF. The final concentrations of EGF were indicated in the graph. (B) The amplitudes of the N-DMR signals, calculated as indicated, as a function of EGF concentration. (C) The time τ for the transition from the P-DMR to the N-DMR event as a function of EGF concentration. (D) The decay constant κ of the N-DMR event as a function of EGF concentration.

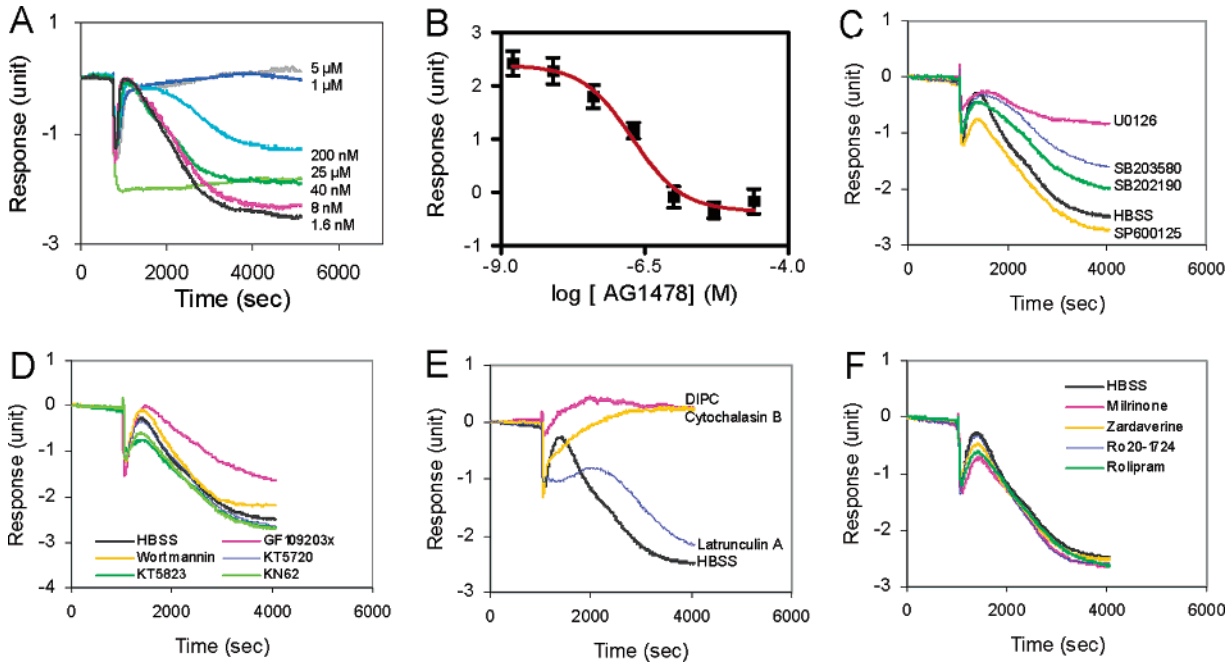

Figure 5. Mechanism of EGF-induced DMR in quiescent A431 cells. (A) Pretreatment of A431 cells with AG1478 led a dose-dependent suppression of the response induced by 32 nM EGF. (B) The amplitudes of the N-DMR signals as a function of AG1478 concentration. Triplicate experiments were used for the statistic calculation. (C) The effect of Ras/MAPK pathway modulators on the EGF-induced response. The modulators were U0126 (1 μM), SB203580 (10 μM), SB202190 (10 μM), and SP600125 (10 μM). (D) The effect of protein kinase inhibitors on the EGF-induced response. The inhibitors were GF109203x (1 μM), wortmannin (1 μM), KT5720 (1 μM), KT5823 (1 μM), and KN62 (10 μM). (E) The effect of cytoskeleton modulators on the EGF-induced response. The modulators were DIPC (50 μM), cytochalasin B (10 μM), Latrunculin A (10 μM). (F) The effect of phosphodiesterase inhibitors on the EGF-induced response. The inhibitors were milrinone (10 μM), Ro 20-1724 (10 μM), (*R*)-(−)-rolipram (10 μM), and zardaverine (10 μM). The cells pretreated with HBSS at the same volume as the compound solution (50 μL) were used as a positive control. The final concentrations were indicated. The concentration of EGF used for all in (a−f) was 32 nM.

inhibits the ERK activation.[25−26] Thus, the N-DMR signals are mainly due to EGF-induced cell detachment and movement, while the U0126-modulated EGF response is possibly related to receptor endocytosis. Conversely, both SB203580 and SB20219 only led to a partial attenuation, whereas SP600125 had little effect on the EGF response. These results suggested that the EGF response primarily involves the Raf-MEK pathway and proceeds through MEK.

We further examined the effect of protein kinase inhibitors on the EGF response, since EGFR signaling involves other protein kinases (Figure 5D). Pretreatment of A431 with wortmainnin (a PI3K inhibitor), KT 5720 (an inhibitor of protein kinase A), KT5823 (an inhibitor of protein kinase G), and KN 62 (an inhibitor of CaM kinase II) showed that these inhibitors had little effect on the response, suggesting that the DMR signal is related to mass redistribution perpendicular to the sensor surface. In contrast, GF 109203x (an inhibitor of protein kinase C) exhibited partial attenuation on the response. These results indicated that modulation of protein kinase C, but not PI3K, protein kinase A, and CaM II, alters the ability of EGF to mediate the DMR changes.

Since the trafficking of proteins and morphological changes of cells require the rearrangement of cytoskeleton structure,[19,27] we examined the effect of cytoskeleton modulators on the DMR response. Pretreatment of A431 with cytochalasin B totally abolished the N-DMR signal but prolonged the P-DMR phase, whereas latrunculin A significantly suppressed both DMR signals with a great delayed transition time (Figure 5E), suggesting that F-actin may regulate EGFR signaling.[27] Although both toxins cause actin disassembly, they act through distinct mechanisms: cytochalasin B caps actin filaments, while latrunculin A sequesters actin monomers. Conversely, neither a stabilizing polymeric F-actin agent phalloidin nor the microtubule disrupters, vinblastine and nocodazole, had any effect on the response (data no shown). These results confirmed that the N-DMR events utilize to less extent the reorganization of preexisting actin than actin polymerization and are independent of microtubule assembly. These results also supported the hypothesis that the P-DMR was at least partially due to the recruitment of intracellular components to the activated receptors, whereas the N-DMR is partially due to receptor endocytosis. This was further suggested by the effect of cell membrane-permeable DIPC (Figure 5E). Dynamin is a key component for receptor endocytosis, and endocytic trafficking of active MEK rather than of activated receptors appears to be critical for ERK activation.[19−20]

Cyclic AMP (cAMP) has served as a paradigm of an intracellular second messenger, and the cAMP pathways cross talk with and attenuate growth factor-stimulated MAP kinase activity.[28−29] Since phosphodiesterases (PDE) regulate the cAMP levels in cells,[30] the role of PDEs on the EGF-induced response was studied using the PDE inhibitors milrinone, Ro 20-1724, (*R*)-(−)-rolipram and zardaverine. None of these inhibitors had observable effects on the responses (Figure 5F), suggesting that cAMP may not be involved in the overall DMR response, or modulation of PDE activity by PDE inhibitors alone may not be sufficient to counteract the Ras/MAPK signal.

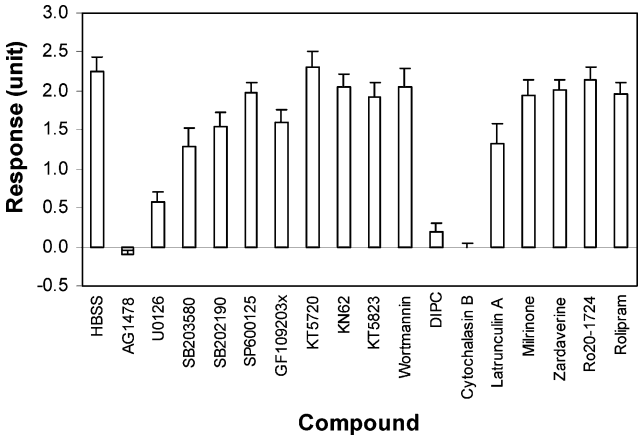

Figure 6. Amplitudes of the N-DMR event in the EGF-induced DMR signal as a function of the compound. The conditions were same as indicated in Figure 5, except for AG1478, which was at 1 μM. The "HBSS" in the graph indicated that the cells were pretreated with 1× HBSS buffer prior to EGF stimulation and used as a positive control. At least two independent experiments for each compound were used for the statistical analysis.

Figure 6 summarized the attenuation of the EGF-induced DMR signals by the modulators examined. The amplitudes of the N-DMR event were plotted as a function of the modulators. Results suggested that modulations of different targets result in distinct attenuations of the DMR signal. Thus, the DMR signatures obtained can provide links of various targets to distinct steps in the cellular responses.

CONCLUSION

We have identified a unique optical signature of dynamic mass redistribution for EGFR signaling mediated by EGF in A431 cells. The DMR signature offers an integrated, quantitative, and dynamic representation of EGFR activation and allows us to map the EGFR signaling pathways. The strong dependence on EGFR kinase activity and MEK1/2, the partial attenuation by p38 MAPK inhibitors and Src-family tyrosine kinase inhibitor, and the little effect of the JNK inhibitor suggest that the Ras/MAPK signaling is a critical element in the EGF-induced DMR events. The DMR changes in A431 appear to be partially PKC mediated, as preincubating cells with GF 109203x led to a partial attenuation. Since there are increasing numbers of mitogenic GPCR agonists that activate the Ras/MAPK pathway through EGFR transactivation,[4] the transactivation may act as a signaling amplification mechanism such that it is possible to apply the novel optical signature to study GPCR signaling in its native environment. Our findings shed new light on the integration of a multitude of signals transduced through a specific molecule and elucidated the importance of the networking interaction(s) among a variety of components in the signaling pathways that determine the cell function and a specific cell response.

(25) Kholodenko, B. N. *J. Exp. Biol.* **2003**, *206*, 2073−2082.
(26) Kranenburg, O.; Verlaan, I.; Moolenaar, W. H. *J. Biol. Chem.* **1999**, *274*, 35301−35304.
(27) Fujimoto, L. M.; Roth, R.; Heuser, J. E.; Schmid, S. L. *Traffic* **2000**, *1*, 161−171.
(28) Dumaz, N.; Light, Y.; Marais, R. *Mol. Cell. Biol.* **2002**, *22*, 3717−3728.
(29) Hafner, S.; Adler, H. S.; Mischak, H. *Mol. Cell. Biol.* **1994**, *14*, 6696−6703.
(30) Conti, M.; Richter, W.; Mehats, C.; Livera, G.; Park, J.-Y.; Jin, C. *J. Biol. Chem.* **2003**, *278*, 5493−5496.

Received for review May 20, 2005. Accepted June 30, 2005.

AC050887N